Relativistic fermionium production by electrons in a crystal

Geir Inge Sandnes and Haakon A. Olsen

Institute of Physics, University of Trondheim, College of Arts and Sciences, N-7055 Dragvoll, Norway
(Received 24 September 1992; revised manuscript received 19 July 1993)

The coherent production of relativistic fermionium by high-energy electrons in a crystal is calculated.
It is shown that considerable enhancement of the cross section occurs at certain angles and energies.

I. INTRODUCTION

The creation of relativistic fermionium, in particular positronium, in high-energy electron collisions with atoms has been calculated in a previous paper [1]. There creation of para- and orthofermionium was discussed and it was shown that for high energies both positronium and μ-fermionium would be created at reasonable rates.

In an interesting paper Kunashenko and Pivovarov [2] have recently used the results from production of positronium by photons on atoms [3] to calculate positronium production in a crystal, obtaining coherent production effects. They show that considerable enhancement occurs for certain angles and energies. We find in the present paper that fermionium production by high-energy electrons in a crystal leads to similar enhancements. In Secs. II and III we obtain production cross sections for parafermionium (singlet, spin zero) and orthofermionium (triplet, spin one), respectively.

II. PRODUCTION
OF PARAFERMIONIUM (SINGLET)

The parafermionium state is produced by the electron-field virtual photon in the field of the atom (Fig. 1), and the process is thus closely related to the production by a real photon [3].

For high energies the cross section is obtained by multiplying the real photon cross section [3] $d\sigma(\gamma Z \to (f\bar{f})Z)$ by the number of virtual photons [4]

$N(\omega)d\omega/\omega$, where $\omega = E_{f\bar{f}}$ is the fermionium energy, and where we neglect the contribution from longitudinal virtual photons, which is a good approximation for high energies. In order to take into account the crystal coherence effect, we further multiply with the usual coherence factor

$$\left| \sum_{n=0}^{N-1} \exp(in\mathbf{q}\cdot\mathbf{d}) \right|^2 = \frac{\sin^2\frac{N}{2}\mathbf{q}\cdot\mathbf{d}}{\sin^2\frac{1}{2}\mathbf{q}\cdot\mathbf{d}} \tag{1}$$

for electrons entering the crystal parallel to a crystal axis. Since the screening radius is considerably smaller than the distance between atoms in the crystal, only strings of atoms parallel to the electron beam contribute to the coherence effect. N is the number of atoms along the string and d is the lattice constant. Lattice vibrations are taken into account in the Debye-Waller theory [5,6], briefly discussed in the Appendix, by the factor

$$e^{-A\mathbf{q}^2} \tag{2}$$

with the Debye-Waller function

$$A = \frac{3m_e^2}{4Mk_B\theta_D}\left[1 + 4\left[\frac{T}{\theta_D}\right]^2 \int_0^{\theta_D/T} \frac{t}{e^t-1}dt\right] . \tag{3}$$

Here T is the temperature, θ_D the Debye temperature, k_B the Boltzmann constant, and M the atomic mass.

The cross section for coherent creation of singlet fermionium in the nth energy level s is thus given by

$$d^2\sigma_{\text{sing}}(E_{f\bar{f}}\theta) = 4\pi\frac{Z^2\alpha^6}{n^3} \frac{\sin^2\left\{N\frac{d}{\lambda_e}\frac{E_{f\bar{f}}}{2m_e}\frac{\beta}{2}\left[\frac{2m_{f\bar{f}}^2}{\beta(1+\beta)E_{f\bar{f}}^2} + 2(1-\cos\theta)\right]\right\}}{\sin^2\left\{\frac{d}{\lambda_e}\frac{E_{f\bar{f}}}{2m_e}\frac{\beta}{2}\left[\frac{2m_{f\bar{f}}^2}{\beta(1+\beta)E_{f\bar{f}}^2} + 2(1-\cos\theta)\right]\right\}} d\theta$$

$$\times \frac{m_{f\bar{f}}^2\sin^3\theta}{\beta E_{f\bar{f}}^4\left[\frac{m_{f\bar{f}}^4}{\beta(1+\beta)^2E_{f\bar{f}}^4} + \frac{\Lambda^2}{\beta E_{f\bar{f}}^2} + 2(1-\cos\theta)\right]^2\left[\frac{2m_{f\bar{f}}^2}{\beta(1+\beta)E_{f\bar{f}}^2} + 2(1-\cos\theta)\right]^2}$$

$$\times \frac{dE_{f\bar{f}}}{E_{f\bar{f}}}\frac{\alpha}{2\pi}\left\{\left[1 + \left[\frac{E_1-E_{f\bar{f}}}{E_1}\right]^2\right]\ln\frac{E_1(E_1-E_{f\bar{f}})m_{f\bar{f}}^2}{E_{f\bar{f}}^2 m_e^2} - 2\frac{E_1-E_{f\bar{f}}}{E_1}\right\}e^{-A\mathbf{q}^2} , \tag{4}$$

where we have used

$$\mathbf{q}\cdot\mathbf{d}=(\mathbf{k}-\mathbf{p}_{f\bar{f}})\cdot\mathbf{d}=(E_{f\bar{f}}-p_{f\bar{f}}\cos\theta)d$$

$$=\tfrac{1}{2}E_{f\bar{f}}\beta\left[\frac{2m_{f\bar{f}}^2}{\beta(1+\beta)E_{f\bar{f}}^2}+2(1-\cos\theta)\right]d \ . \tag{5}$$

Here E_1 is the initial electron energy and β the velocity, m_e and $m_{f\bar{f}}$ the electron and fermionium masses, respectively, λ_e the Compton wavelength, $\Lambda^{-1}=121Z^{-1/3}m_e^{-1}$ is the Molière screening radius, and θ the emission angle of the fermionium. The vectors k and p are the virtual photon and fermionium momenta, respectively.

For high energies the fermionium is emitted at small angles, and the cross section summed over all energy levels becomes

$$d^2\sigma_{\text{sing}}(E_{f\bar{f}},\theta)=4\pi Z^2\alpha^6\zeta(3)\frac{m_{f\bar{f}}^2\theta^3}{E_{f\bar{f}}^4\left[\frac{m_{f\bar{f}}^4}{4E_{f\bar{f}}^4}+\frac{\Lambda^2}{E_{f\bar{f}}^2}+\theta^2\right]\left[\frac{m_{f\bar{f}}^2}{E_{f\bar{f}}^2}+\theta^2\right]^2}\frac{\sin^2 N\dfrac{d}{\lambda_e}\dfrac{E_{f\bar{f}}}{2m_e}\dfrac{1}{2}\left[\dfrac{m_{f\bar{f}}^2}{E_{f\bar{f}}^2}+\theta^2\right]}{\sin^2\dfrac{d}{\lambda_e}\dfrac{E_{f\bar{f}}}{2m_e}\dfrac{1}{2}\left[\dfrac{m_{f\bar{f}}^2}{E_{f\bar{f}}^2}+\theta^2\right]}d\theta$$

$$\times\frac{dE_{f\bar{f}}}{E_{f\bar{f}}}\frac{\alpha}{2\pi}\left\{\left[1+\left[\frac{E_1-E_{f\bar{f}}}{E_1}\right]^2\right]\ln\frac{E_1(E_1-E_{f\bar{f}})m_{f\bar{f}}^2}{E_{f\bar{f}}^2 m_e^2}-2\frac{E_1-E_{f\bar{f}}}{E_1}\right\}e^{-A\mathbf{q}^2} \tag{6}$$

with $\zeta(p)=\sum n^{-p}$ the Riemann ζ function, $\zeta(3)=1.202$.

The break-up effect [3,7] of fermionium in the crystal limits the effective number of atoms in the string. An approximation for the effective thickness of the target for positronium production is

$$L=(p\sigma_b)^{-1} \ ,$$

with $\sigma_b\approx3.5Z^{4/3}10^{-20}$ cm^2, and ρ the number of atoms per cm^3. For μ-fermionium $(\mu\bar{\mu})$ production the corresponding break-up cross section is $\sigma_b\approx1.3Z^210^{-23}$ cm^2.

We have calculated positronium production in a Cu crystal, $d=3.61$ Å. We use simplified Molière [8] screening, with screening radius $\Lambda^{-1}=121Z^{-1/3}m_e^{-1}$, and the effective number of atoms in the string for producing positronium $N=100$. We show in Fig. 2(a) an example of angular dependence of positronium emission. For positronium energy 80 MeV, a strong emission of positronium occurs in a cone with an opening angle $\theta\approx20$ mrad in addition to the strong forward, $\theta\leq4$ mrad, emission.

It is true that the wide positronium spectrum may reduce an angular effect due to the crystal coherence effect. For the case of very narrow angular peaks, however, as for example in Fig. 2(a) for $\hat{\theta}\approx0.8$, the peak moves very little with positronium energy. In fact it can be shown that the peak occurs for positronium energies between 70 and 200 MeV within a narrow interval of θ between 17.6 and 21 mrad.

In Fig. 2(b) the cross section integrated over angles, normalized to unity

$$F(x)=\frac{d\sigma/dx}{\sigma} \tag{7}$$

is given, with $x=E_{\text{Ps}}/E_1$, and E_{Ps} the positronium energy. In comparison the cross section for production on a single atom [1] is given, normalized in the same way. In Table I the corresponding total cross sections for coherent and incoherent positronium production are given for some initial electron energies.
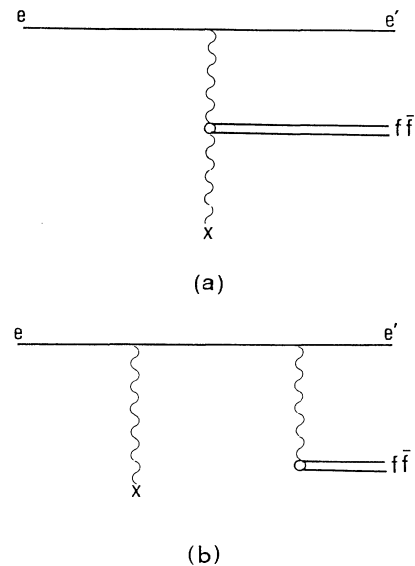

(a)

(b)

FIG. 1. Singlet (a) and triplet (b) production of a bound $f\bar{f}$ state in a collision of an electron with an atom.

TABLE I. Total cross sections for electroproduction of singlet positronium per target atom, in units of $1.20Z^2\alpha^5r_e^2$, for production in a Cu crystal, σ_{coh}, and on a single Cu atom, σ_{incoh}.

E_1	σ_{coh}	σ_{incoh}	$\sigma_{\text{coh}}/\sigma_{\text{incoh}}$
20 MeV	0.6426	0.5063	1.269
100 MeV	2.5264	2.2744	1.111
1 GeV	8.1176	7.2741	1.116

III. PRODUCTION OF ORTHOFERMIONIUM (TRIPLET)

The cross section for triplet fermionium production is obtained by multiplying the single-atom cross section [1], by the coherence factor, Eq. (1), and the thermal factor of Eq. (2)

$$d^5\sigma_{\text{trip}}(\mathbf{p}_2,\mathbf{p}_{f\bar{f}}) = -2\frac{Z^2\alpha^7}{(2\pi)^2}\frac{\zeta(3)}{E_1E_2E_{f\bar{f}}}\frac{[1-F(\mathbf{q})]^2}{\mathbf{q}^4}$$

$$\times\left[\frac{\mathbf{q}^2}{D_1D_2}(E_1^2+E_2^2)-\frac{1}{4}\left[\frac{D_1}{D_2}+\frac{D_2}{D_1}\right]+(2m_e^2+m_{f\bar{f}}^2)\left[\frac{E_1}{D_2}+\frac{E_2}{D_1}\right]^2\right]$$

$$\times\frac{\sin^2\frac{N}{2}\mathbf{q}\cdot\mathbf{d}}{\sin^2\frac{1}{2}\mathbf{q}\cdot\mathbf{d}}\frac{d^3p_{f\bar{f}}d^3p_2}{dE_2}e^{-A\mathbf{q}^2}, \tag{8}$$

(a)

$$\frac{d^2\sigma}{dxd\hat{\theta}}$$

(cm^2/rad)

$\hat{\theta}$ (rad)

(b)

F

$x = E_{Ps}/E_1$

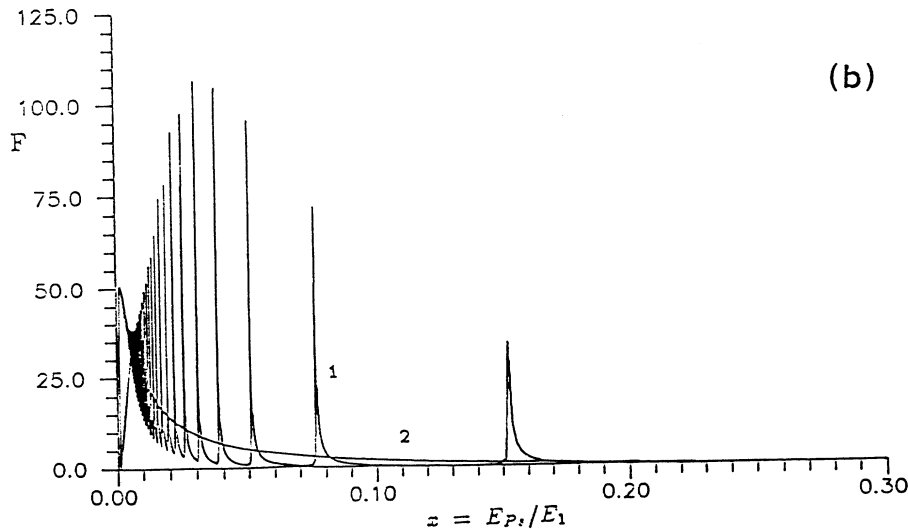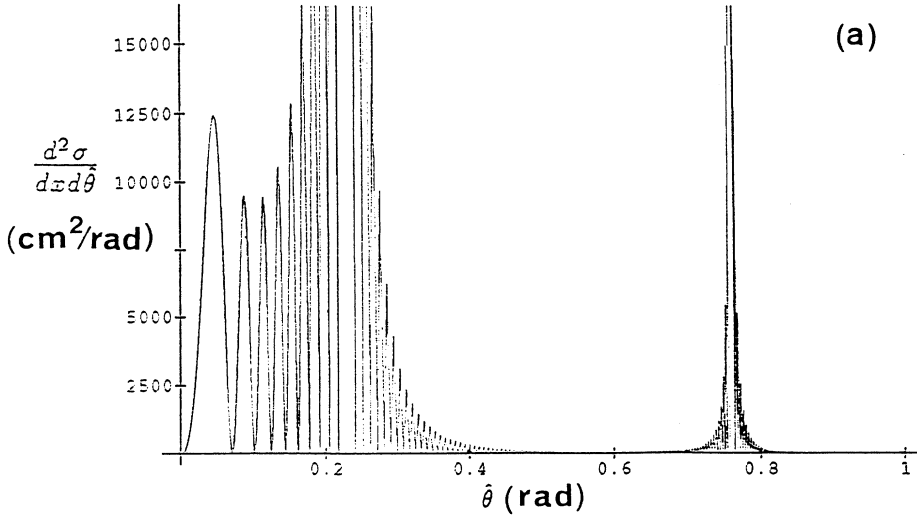FIG. 2. Singlet positronium: (a) Angular distribution in units of $1.20Z^2\alpha^5r_e^2$ for a Cu lattice, $N=100$, $E_1=1$ GeV, $E_{\text{Ps}}=80$ MeV, $T=0$, $\hat{\theta}=\theta E_{\text{Ps}}/m_{\text{Ps}}c^2$. The height of the peak at $\hat{\theta}=0.76$ is 3.3×10^5, and at $\hat{\theta}=0.21$ it is 4.1×10^7. (b) Energy spectrum normalized to unity for $E_1=100$ MeV, $T=0$. Curve 1, Cu lattice, $N=100$. Curve 2, Single Cu atom.

where we again use the Molière approximation [8] for the screening factor $F(q)$. It is convenient to choose the z axis along p_1, then

$$\mathbf{q \cdot d} = q_z d \approx d \left[q_{\min} + \frac{v^2}{2E_2} + \frac{u^2}{2E_{f\bar{f}}} \right] \tag{9}$$

is independent of the azimuthal angles ϕ_2 and $\phi_{f\bar{f}}$ which makes integration over these angles possible.

In Eq. (9) u and v are the components of p_2 and $p_{f\bar{f}}$ perpendicular to p_1, respectively, and the minimum momentum transfer

$$q_{\min} = \frac{m_e^2 E_{f\bar{f}}^2 + m_{f\bar{f}}^2 E_1 E_2}{2E_1 E_2 E_{f\bar{f}}} . \tag{10}$$

Further, the functions D_1 and D_2 are for the actual case of small angles, given by

$$D_1 = m_{f\bar{f}}^2 - 2p_1 p_{f\bar{f}} = - \left[2E_2 q_{\min} + \frac{E_1}{E_{f\bar{f}}} u^2 \right] ,$$

$$D_2 = m_{f\bar{f}}^2 + 2p_2 p_{f\bar{f}} = 2E_1 q_{\min} + \frac{E_{f\bar{f}}}{E_2} v^2 + \frac{E_2}{E_{f\bar{f}}} u^2 - 2uv \cos(\phi_2 - \phi_{f\bar{f}}) .$$

In these expressions for D_1 and D_2, p_1, p_2, and $p_{f\bar{f}}$ are four vectors.

The ϕ_2 and $\phi_{f\bar{f}}$ integrations give the result

$$d^3\sigma_{\text{trip}}(\mathbf{p}_2, \mathbf{p}_{f\bar{f}}) = Z^2 \alpha^5 \zeta(3) r_f^2 \frac{2m_f^2}{E_1 E_2 E_{f\bar{f}}} \frac{\sin^2 \frac{N}{2} \mathbf{q \cdot d}}{\sin^2 \frac{1}{2} \mathbf{q \cdot d}} e^{-A\mathbf{q}^2}$$

$$\times \left\{ \frac{E_1^2 + E_2^2}{(-D_1)(c+d)^2} \left[\frac{(ca-b^2)(c+d)}{(c^2-b^2)^{3/2}} - \frac{\Lambda^2}{\sqrt{c^2-b^2}} + \frac{a+d}{\sqrt{d^2-b^2}} \right] \right.$$

$$- \frac{1}{4} \left[\frac{(-D_1)}{(c+d)^2} \left[\frac{c(2c+d)-b^2}{(c^2-b^2)^{3/2}} + \frac{1}{\sqrt{d^2-b^2}} \right] + \frac{1}{(-D_1)} \frac{cd+b^2}{(c^2-b^2)^{3/2}} \right]$$

$$- (2m_e^2 + m_{f\bar{f}}^2) \left[\frac{E_1^2}{(c+d)^3} \left[\frac{c(3c+d)-2b^2}{(c^2-b^2)^{3/2}} + \frac{d(3d+c)-2b^2}{(d^2-b^2)^{3/2}} \right] \right.$$

$$- \frac{2E_1 E_2}{(-D_1)(c+d)^2} \left[\frac{c(2c+d)-b^2}{(c^2-b^2)^{3/2}} + \frac{1}{\sqrt{d^2-b^2}} \right]$$

$$\left. \left. + \frac{E_2^2}{(-D_1)^2} \frac{c}{(c^2-b^2)^{3/2}} \right] \right\} u \, du \, v \, dv \, dE_{f\bar{f}} \tag{11}$$

with

$$a = q_z^2 + u^2 + v^2 = \left[q_{\min} + \frac{E_1}{2E_2 E_{f\bar{f}}} u^2 \right]^2 + u^2 + v^2 ,$$

$$b = 2uv ,$$

$$c = a + \Lambda^2 ,$$

$$d = 2E_1 q_{\min} + \frac{E_2}{E_{f\bar{f}}} u^2 + \frac{E_{f\bar{f}}}{E_2} v^2 .$$

We give in Figs. 3(a) and 3(b) the angular distribution $G(\hat{\theta})$, the differential cross section in $\hat{\theta}$, and E_{Ps} normalized to unity, for production of triplet positronium in a Cu lattice.

$$G(\hat{\theta}) = \frac{d^2\sigma}{dE_{\text{Ps}} d\hat{\theta}} \bigg/ \int_0^2 \frac{d^2\sigma}{dE_{\text{Ps}} d\hat{\phi}} d\hat{\phi} . \tag{12}$$

For comparison, the cross section for production on a single atom, normalized in the same way, is given. As for the case of singlet production, triplet positronium is emitted in marked cones for each positronium energy.
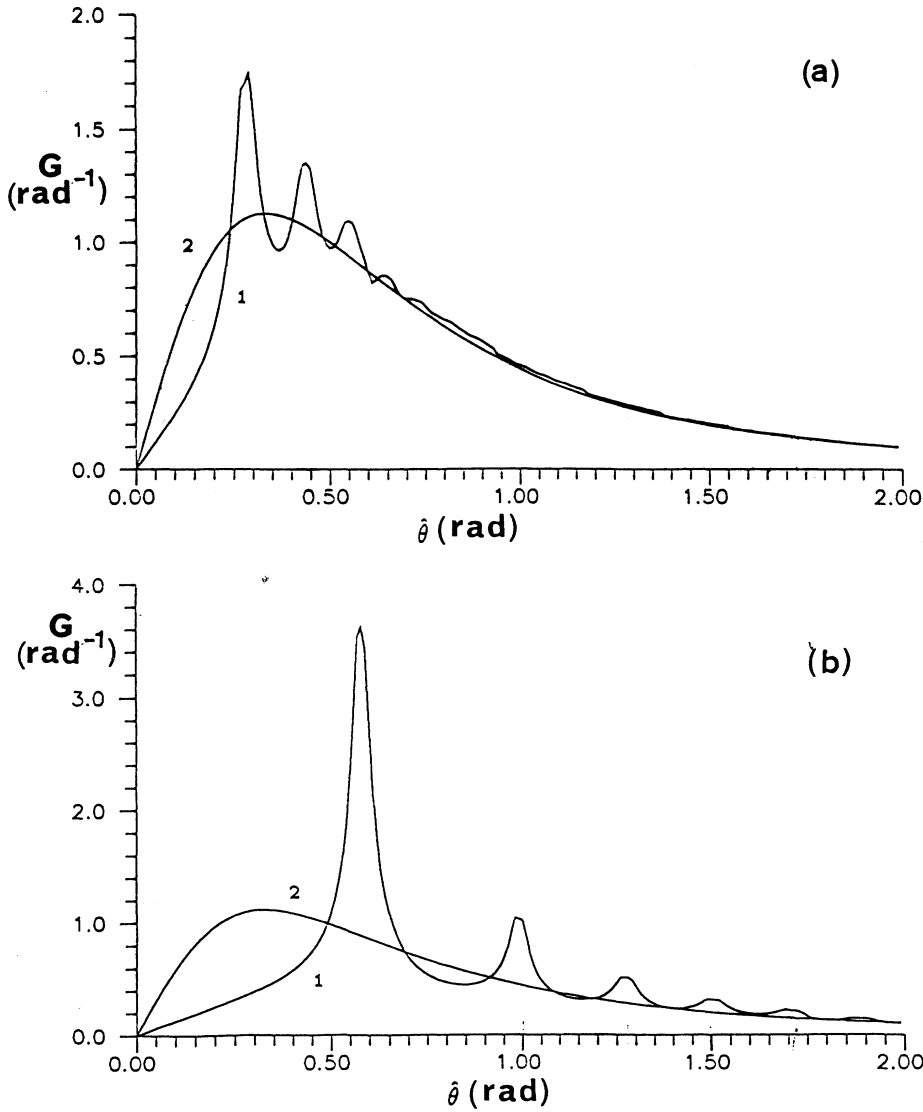
FIG. 3. Triplet positronium. Angular distribution normalized to unity, $\hat{\theta} = \theta E_{Ps}/m_{Ps}c^2$. Curve 1, Cu lattice, $N = 100$, $T = 0$. Curve 2, single Cu atom. (a) $E_1 = 100$ MeV, $E_{Ps} = 78$ MeV. (b) $E_1 = 1$ GeV, $E_{Ps} = 890$ MeV.

IV. DISCUSSION

We have shown that, as for the case of fermionium produced by photons [2], the crystal effect gives strong enhancements for certain energies and angles for fermionium produced by electrons. For singlet fermionium production the electron and photon production are in fact closely related, as can be seen from Eq. (4). The cross section is proportional to the virtual electron-photon cross section, the first two factors of Eq. (4), folded into the virtual photon energy distribution. The peaks shown in the positronium energy spectrum, in Fig. 2(b), are therefore closely related to the peaks obtained by Kunashenko and Pivovarov [2], although the form of the spectrum is quite different.

Triplet fermionium is produced in electron-atom collisions, not in photon-atom collisions. In contrast to singlet fermionium production, triplet fermionium is produced in electron-atomic collisions preferably with high energy. This may be seen from the following simple ar-

gument. The cross section integrated over values of the momentum transfer q gives essentially proportionality to q_{min}^{-1},

$$\int_{q_{min}}^{q_{max}} d^3q/q^4 \sim q_{min}^{-1} .$$ (13)

With q_{min} given by Eq. (10), the spectrum is proportional to

$$d\sigma(E_{f\bar{f}})/dE_{f\bar{f}} \sim q_{min}^{-1} \sim \left[1 - \frac{E_{f\bar{f}}}{E_1} + \left[\frac{m_e E_{f\bar{f}}}{m_{f\bar{f}} E_1} \right]^2 \right]^{-1}$$ (14)

which gives a strong enhancement for higher fermionium energies. As discussed previously [1], production of triplet positronium provides possibilities for obtaining high energy—thereby semistable positronium beams in the laboratory system. The enhancements at certain angles and energies which occur when the production process

takes place in a crystal may increase the possibility for obtaining such beams.

It should be noted that the positronium production effect described here differs from the crystal-assisted pair-creation effect described by Kimball *et al.* [9]. In fact positronium could not be produced by their mechanism, since an electron bound in positronium can not give "bound states" in the crystal.

APPENDIX

Temperature, and even zero point oscillations, may have effects on the lattice which can lead to changes in the cross sections for fermionium production [10]. The temperature effect is most easily obtained by the use of the well-known Debye-Waller theory. This theory was developed for x-ray Bragg reflection in crystals [5,6] and gives the damping of the intensity, with A given in Eq. (3),

$$I(T) = I(0)\exp\{-A[2(\sin\theta/2)/\lambda]^2\}$$

with θ the x-ray-scattering angle and λ the wavelength. Since $2(\sin\theta/2)/\lambda = q$, the damping factor depends only

on the momentum transfer to the lattice atom, not on the properties of the scattered particles.

The lattice vibrations are thus taken into account by multiplication with the damping factor Eq. (2), and the cross section for coherent production of fermionium at the temperature T is given by

$$d\sigma_{\text{coh}} = \frac{\sin^2\frac{N}{2}\mathbf{q}\cdot\mathbf{d}}{\sin^2\frac{1}{2}\mathbf{q}\cdot\mathbf{d}}e^{-Aq^2}d\sigma_{f\bar{f}} \tag{A1}$$

with $d\sigma_{f\bar{f}}$ the single-atom production cross section. In addition, fermionium is produced by the number of atoms $N[1-\exp(-Aq^2)]$ taking part in the incoherent process,

$$d\sigma_{\text{incoh}} = N[1-\exp(-Aq^2)]d\sigma_{f\bar{f}} . \tag{A2}$$

For Cu, $A(T)q^2$ is very small for $T=0$. For the largest values of $q \sim \Lambda$, one finds

$$A(0)q^2 \sim 0.07 . \tag{A3}$$

The damping is therefore very small, and the number of incoherently produced fermionium particles is negligible.

---

[1] Egil Holvik and Haakon A. Olsen, Phys. Rev. D **35**, 2124 (1987).

[2] Yu. Kunashenko and Yu. L. Pivovarov, Yad. Fiz. **51**, 627 (1990) [Sov. J. Nucl. Phys. **51**, 397 (1990)].

[3] H. A. Olsen, Phys. Rev. D **33**, 2033 (1986); V. L. Lyuboshits, Yad. Fiz. **45**, 1099 (1987) [Sov. J. Nucl. Phys. **45**, 682 (1987)].

[4] H. A. Olsen, Phys. Rev. D **19**, 100 (1979).

[5] I. Waller, Z. Phys. **17**, 398 (1923).

[6] See, e.g., M. Blackman, in *The Specific Heat of Solids* in *Handbuch der Physik VII*, edited by S. Flügge (Springer-Verlag, Berlin, 1955).

[7] L. S. Dulyan, Ar. M. Kotsinyan, and R. N. Faustov, Yad. Fiz. **25**, 814 (1977) [Sov. J. Nucl. Phys. **25**, 434 (1977)]; St. Mrówczyński, Phys. Rev. A **33**, 1549 (1986).

[8] G. Molière, Z. Naturforsch. Teil A **2**, 133 (1947).

[9] J. C. Kimball, N. Cue, L. M. Roth, and B. B. Marsh, Phys. Rev. Lett. **50**, 950 (1983).

[10] For a simplified model, see [2]. See also H. Überall, Phys. Rev. **103**, 1055 (1956).